FEBS Letters 581 (2007) 2974–2980

Tight junction modulation and biochemical characterisation of the zonula occludens toxin C-and N-termini

E. Schmidt[a], S.M. Kelly[b], C.F. van der Walle[a,*]

[a] *Institute of Pharmacy and Biomedical Sciences, University of Strathclyde, 27 Taylor Street, Glasgow, UK*
[b] *Biochemistry and Molecular Biology, Davidson Building, University of Glasgow, UK*

Received 5 March 2007; revised 27 April 2007; accepted 17 May 2007

Available online 29 May 2007

Edited by Gianni Cesareni

Abstract The ZOT N-terminal domain was expressed and refolded, yielding a soluble protein with defined secondary structure. Although distantly related to protein I of filamentous phages, no evidence of ATPase activity was found. It is therefore unlikely that the ZOT N-terminal domain is involved in cholera toxin phage packaging in *Vibrio cholerae*. The ZOT C-terminal domain caused delocalisation of occludin and ZO-1 from Caco-2 cell–cell contacts, irrespective of disulfide bridge formation in its putative binding domain. However, the C-terminal domain did not cause actin reorganisation and this may explain the absence of a concomitant reduction in the transepithelial electrical resistance across cell monolayers.

Keywords: Tight junction; Zonula occludens toxin; ATPase

1. Introduction

Zonula occludens toxin (ZOT) is a 399 amino acid enterotoxin expressed by *Vibrio cholerae*. ZOT is predicted to have a single transmembrane region between residues 226–246; the 153-residue ZOT C-terminal domain (ZOT-CT) facing the bacterial periplasm with the 225-residue ZOT N-terminal fragment (ZOT-NT) residing in the cytoplasm [1]. ZOT-CT is a minor toxin which transiently loosens the intercellular tight junctions [2] following binding to a putative receptor localised to the cell periphery [3]. A cysteine pair in ZOT-CT (Cys^{288} and Cys^{293}) leads into the putative ZOT receptor binding domain (G^{290}RLCVQDG) [4]. The presence of a disulfide bridge between Cys^{288} and Cys^{293} would constrain the conformation of the binding domain and may affect tight junction modulation. We were therefore prompted to investigate the role of the redox state of the cysteine pair in relation to ZOT-CT function.

The *zot* gene is encoded on the CTXΦ plasmid that carries the major pathogens Cholera Toxin A and B, and has been suggested to have evolved from gene product I (pI) of a Pf1-bacteriophage [1]. The evidence for this arose from alignment of the ZOT-NT with the equivalent open reading frames of pI for filamentous phages, themselves putative NTPases. Three regions were identified in ZOT-NT that resemble pI: a modified A-motif (the hydrophobic β-strand binding substrate), a B-motif typical of viral NTPases [5] and a C-motif conserved between pI of filamentous coliphages [6] (Fig. 1).

pI is known to have a single transmembrane domain, yielding a 253 residue N-terminus (similar to ZOT-NT) and a 75 residue cytoplasmic C-terminus (around half the size of ZOT-CT) [7]. In contrast to ZOT, pI is not known to modulate tight junction integrity. Rather, pI has been proven to be involved in the assembly of filamentous phage [8], and its homology to NTPases would suggest that this process requires ATP hydrolysis. Phage assembly and exit from the cell also requires pXI, an in-frame internal translation product of gene I encompassing residues 241–348 of pI [9], pIV oligomers which form a transmembrane pore gating phage extrusion and reduction by (host) thioredoxin [10]. To investigate the role of the ZOT-NT in CTX-phage packaging in *V. cholerae* it was necessary to overcome known problems with the expression of ZOT [3]. Here, we demonstrate a suitable expression system which yields soluble, refolded ZOT-NT and investigate its structure and ATPase activity.

2. Materials and methods

2.1. Cloning procedures

The construction and cloning the *zot* gene has been described previously [3]. Primer pairs 5′-GAGGATCCATCTTTATTCATCACGGCGCG (fwd) and 5′-TAGAAGCTTCTCGAGTTACGTGTCGCGTGCTTTGCC were used to subclone *zot-nt* into pQE80-L (Invitrogen, UK) at BamHI and HindIII sites, and 5′-TAGCCATGGACGGATCCTCGTTTTACGGCTTACACG (fwd) and 5′-TAGGAATTCAAGCTTAAAATATACTATTTAGTCCTTTTTTATC to subclone *zot-ct* into pMAL-c2x (New England Biolabs, UK) at BamHI and HindIII sites. The base sequence and in frame ligation of DNA cassettes was confirmed by DNA-sequencing.

2.2. Expression and purification

pQE80-L/ZOT-NT was expressed as the histidine-tagged fusion protein in *E. coli* strain UT5600 grown at 22 °C in Lennox broth containing 100 μg/ml ampicillin. pMAL-c2X/ZOT-CT was expressed as the maltose binding protein (MBP) fusion product in *Escherichia coli* strain TB1 grown at 22 °C in Terrific containing 100 μg/ml ampicillin. Cells were grown to an OD_{600} of 0.6, expression induced with 0.1 mM isopropyl β-D-1-thiogalactopyranoside and harvested 16 h later. Cells were lysed by sonication and clarified by centrifugation. Supernatent containing ZOT-NT was loaded onto 5 ml Ni^{2+}-Sepharose (GE Healthcare, UK) and eluted with 250 mM imidazole, pH 8. Supernatent containing ZOT-CT was loaded onto amylose-Sepharose (New England Biolabs, UK) and eluted with 10 mM maltose. Protein purity was assessed by Coomassie staining of gels run in a sodium dodecyl sulphate–polyacrylamide gel electrophoresis (SDS–PAGE) system. Concentrations of ZOT-NT and ZOT-CT were determined at A_{280}

*Corresponding author. Fax: +44 0 141 552 2562.
E-mail address: chris.walle@strath.ac.uk (C.F. van der Walle).

0014-5793/$32.00
doi:10.1016/j.febslet.2007.05.051

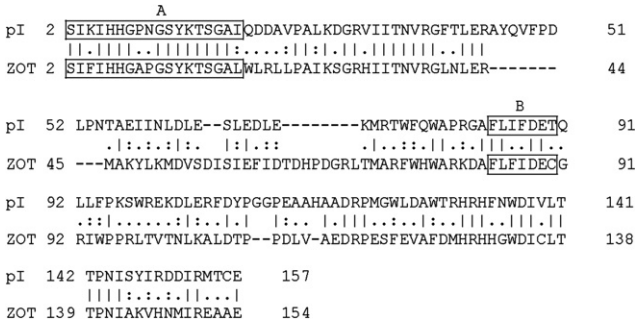

Fig. 1. Alignment of the ZOT N-terminal domain with protein I from Pseudomonas phage Pf1 (locus P25131), using the program "needle" with the EBLOSUM62 matrix. Verticle lines show identical amino acids, colons and full-stops show conserved and semi-conserved amino acids, respectively. The Walker A and B consensus motifs of the NTPase family are boxed.

with calculated molar extinction coefficients of 33 570 and 83 780 (the MBP fusion) M^{-1} cm^{-1}, respectively. ZOT-NT was refolded following precipitation with 70% w/v $(NH_4)_2SO_4$ and solubilisation in 6 M guanidine. HCl (GuHCl) by 100-fold dilution in 100 mM NaOAc pH 4.8.

2.3. Fluorescence measurements

Equilibrium chemical denaturation of ZOT-NT was performed for GuHCl unfolding with measurement of the change in tryptophan (Trp) fluorescence intensity and emission wavelength (λ_{ex} = 295 nm) [11]. Data were fitted to a two-state model of protein unfolding for the calculation of the Gibbs free energy (ΔG) between the folded and unfolded states, extrapolated to 0 M GuHCl to obtain the conformational stability of the protein, $\Delta G_{(H_2O)}$ [12].

2.4. Circular dichroism (CD)

Spectra were recorded on a JASCO J-810 spectropolarimeter for ZOT-NT in 10 mM NaOAc pH 4.8 at a concentration of 0.53 mg/ml. CD measurements were made in quartz cylindrical cells of path length 0.02 cm and 0.5 cm for far and near UV regions, respectively. Mean residue ellipticity values were calculated for a mean residue M_w of 113.5.

2.5. Ellman's (DNTB) assay

The extinction coefficient (ε) for 5,5′-dithio-bis(2-nitrobenzoicacid) (DTNB) (Sigma–Aldrich, UK) was experimentally determined for titration against DTT. Briefly, aliquots of 0.2 mM DTT or protein were added to 1.7 mM DTNB in 50 mM sodium phosphate, 0.1 mM EDTA, pH 8.2. The analysis of ZOT-NT was performed with the addition of 6 M GuHCl. Chromophoric reaction was determined as the absorbance at 412 nm.

2.6. ATPase activity

ZOT-NT (9 μM) or porcine ATPase (40 mU/ml – as the positive control) were incubated with 1.3 mM adenosine 5′-triphosphate (ATP) for 15 min at 37 °C in 100 mM acetate, 0.57 mM EDTA, 5 mM $MgCl_2$, 133 mM NaCl, 3 mM KCl, pH 4.8. Reactions were stopped by addition of 2% trichloroacetic acid and the release of inorganic phosphate was determined by colorimetric reaction with malachite green (Bioassay Systems, UK), recording the absorbance from 400 to 800 nm. To assay the activity of the reduced protein, a 50-fold molar equivalent of tris[2-carboxyethyl] phosphine (TCEP) was added to the incubation mixtures above.

2.7. Cell culture and immunofluorescence microscopy

Caco-2 human colon adenocarcinoma cells were cultivated in high glucose Dulbecco's modified essential medium (DMEM) supplemented with 10% foetal calf serum (FCS) and 2 mM Glutamax (Invitrogen). Adherent cells were grown in Corning 75 cm^3 flasks and subcultured twice weekly with Trypsin-EDTA 0.25%. Experiments were performed between passage 10 and 20.

2.8. Confocal laser scanning microscopy (CLSM)

Caco-2 cells were seeded at 1×10^5 cells/ml onto cover slips in a 24-well plate. On day 7 cells were incubated with oxidised or reduced ZOT-CT (8.3 μM), Cytochalasin D (2 μM, positive control) or MBP (8.3 μM, negative control) for 60 min. (disulfide reduction of ZOT-CT was achieved with dithiothreitol followed by reaction with iodoacetamide and desalting.) Cells were then fixed, permeabilized and non-specific binding blocked with 1% BSA during overnight incubation with mouse anti-occludin and mouse anti-ZO-1 FITC antibody (5 μg/ml, Zymed, UK) at 4 °C in a moist chamber; F-actin was stained using FITC-phalloidin (2 μg/ml) in PBS with 1 h staining. Cells were subsequently rinsed, mounted and viewed.

2.9. Measurement of cell monolayer transepithelial electrical resistance (TEER) and permeability

Caco-2 cells were seeded at 1×10^5 cells/ml onto 12-well polycarbonate membrane (0.4 μm pore diameter) Transwell™ plates (Corning) in complete media supplemented with penicillin (100 U/ml) and streptomycin (0.1 mg/ml). Monolayers were grown between 14 and 21 days until the TEER measurements were 300–600 Ω. Monolayers were then incubated in media containing oxidised or reduced ZOT-CT (8.3 μM), MBP (8.3 μM), or EDTA (30 mM, positive control) for 120 min, and the TEER measured at 20 min intervals (Epithelial-voltohmmeter, World Precisison Instruments, UK). Experiments were performed in triplicate and the data expressed as the means ± standard deviation. Statistical analysis of the change in TEER for each group was performed by one-way ANOVA with Bonferroni's post-test. A significance level of $P < 0.05$ was used to denote significance in all cases.

Fluoresceine-labelled dextran (FITC-dextran 4000) is an impermeable marker to Caco-2 cell monolayers and has been previously used for the study of ZOT [13]. Caco-2 cell monolayers were grown on Transwell™ plates as above and incubated with EDTA (30 mM), MBP (8.3 μM) and oxidised ZOT-CT (8.3 μM) for 1 h, and the TEER measured. Cells were then washed in PBS and incubated with EDTA, MBP or oxidised ZOT as above but with the addition of FITC-dextran 4000 (2.5 mM). Samples were taken from the basolateral compartment at 1 and 2 h and the concentration of FITC-dextran 4000 measured by fluorescence ($\lambda_{ex/em}$ = 495/525 nm).

3. Results

3.1. Structural analysis of ZOT-NT and ATPase activity

SDS–PAGE analysis of the purified ZOT-NT showed a single major band at ~24 kDa (Fig. 2). Trypsin digest and mass spectrometry peptide fragment analysis confirmed the expected peptide sequences. ZOT-NT eluted from the nickel column in pH 8 buffer slowly precipitated over around 1 h on standing at room temperature. The precipitate did not redissolve on dilution, so ZOT-NT was further precipitated in $(NH_4)_2SO_4$ and refolded in pH 4.8 buffer, and remained stable. The CD spectrum for the refolded ZOT-NT was largely dominated by β-sheet/β-turn secondary structure: having relatively weak positive ellipticities below 200 nm and a strong negative ellipticity around 205 nm (Fig. 3). A secondary, weak minimum around 220 nm suggested minor contribution from α-helical structure. This was confirmed with Dichroweb analysis of the CD spectrum for ZOT-NT [14], calculating 19% helical, 25% β-strand, 23% β-turn and 32% unordered structure according to CDSSTR database [15].

During equilibrium chemical denaturation, one transition was observed as a decrease in fluorescence intensity and red shift of the peak maxima emission wavelength (Fig. 4A and B). This suggested that ZOT-NT unfolding involved increased solvent exposure of Trp residues. Fitting the data to a two-state unfolding model gave calculated $[GuHCl]^{\frac{1}{2}}$ of 2.25 M, $\Delta G_{(H_2O)}$ of 3.3 kcal/mol and m (the measure of

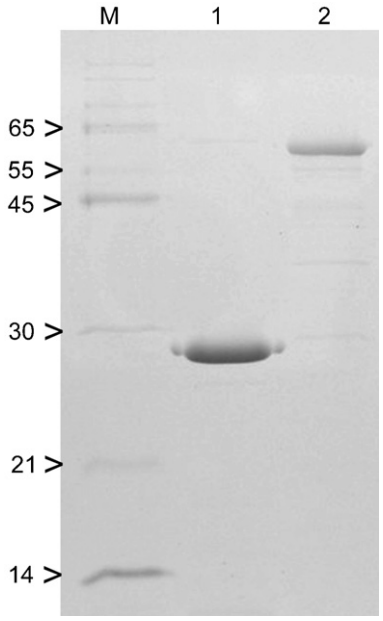

Fig. 2. SDS–PAGE analysis of the purified ZOT-NT and ZOT-CT (as the MBP-fusion). Lane M, protein markers indicated in kDa; lane 1, purified ZOT-NT; lane 2, purified ZOT-CT.

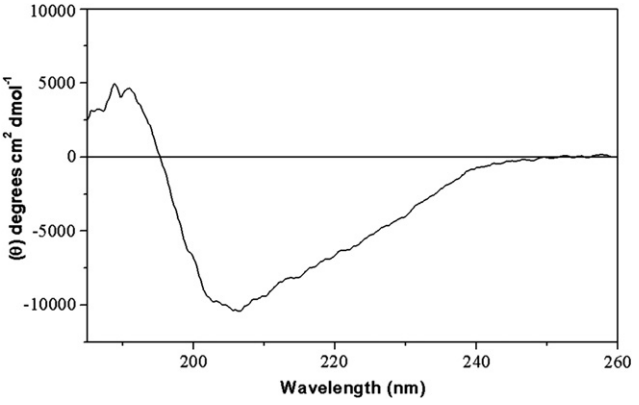

Fig. 3. Circular dichroism spectrum for the refolded ZOT-NT in the far-UV region.

dependence of unfolding on [GuHCl]) of 1.5 kcal/mol/M (Fig. 4A, inset).

The redox state of the cysteine pair was determined using Ellman's assay. The DTNB reaction requires alkaline conditions which precipitate ZOT-NT (pI 9.9) so 6 M GuHCl was added to maintain protein solubility. (ε for DTNB in GuHCl was determined as 11 800 M^{-1} cm^{-1}, similar to the literature values for DTNB in 8 M urea [16]). Measurements under these conditions showed that the refolded ZOT-NT had no free thiol-groups, i.e. the Cys^{89}–Cys^{135} pair was disulfide bridged. While ATPase activity for porcine cerebral cortex ATPase (positive control) was clearly observed, no ATPase activity was observed for ZOT-NT, in either oxidised or reduced states (Fig. 5).

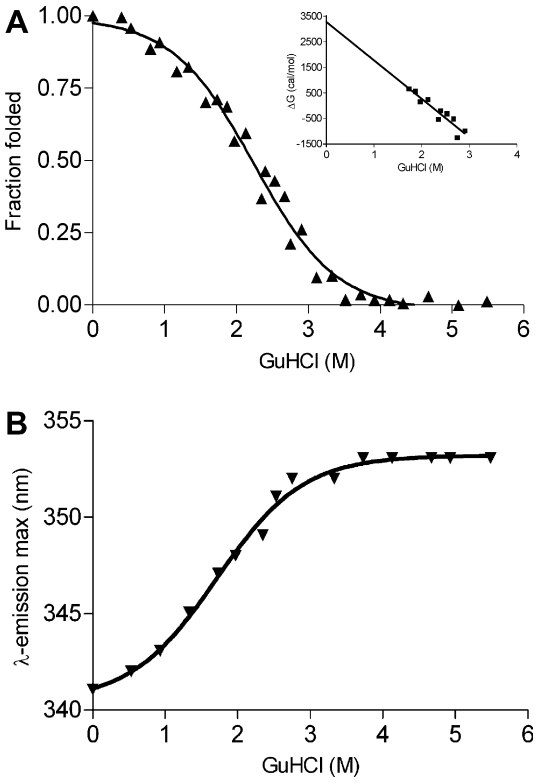

Fig. 4. Equilibrium chemical denaturation of ZOT-NT. (A) Change in fluorescence intensity (as the fraction folded); inset: linear regression analysis for the calculation of $\Delta G_{(H_2O)}$. (B) Change in the fluorescence emission maxima.

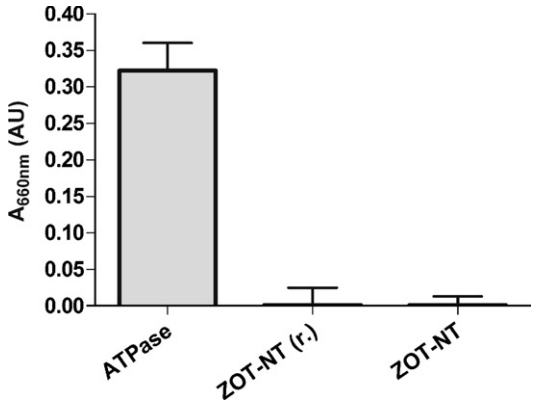

Fig. 5. ATPase activities for reduced (r.) and oxidised ZOT-NT, measured against a positive control (porcine ATPase).

3.2. Tight junction modulation by ZOT-CT does not involve actin reorganisation

Expression and purification of ZOT-CT was confirmed by a single major band by SDS–PAGE (~60 kDa, MBP fusion, Fig. 2) and mass spectrometry analysis of peptide fragments following Trypsin digest. Using Ellman's assay, ZOT-CT was found to contain no free thiol groups, i.e. the cysteine pair formed a disulfide bridge (GuHCl was not added: ZOT-CT

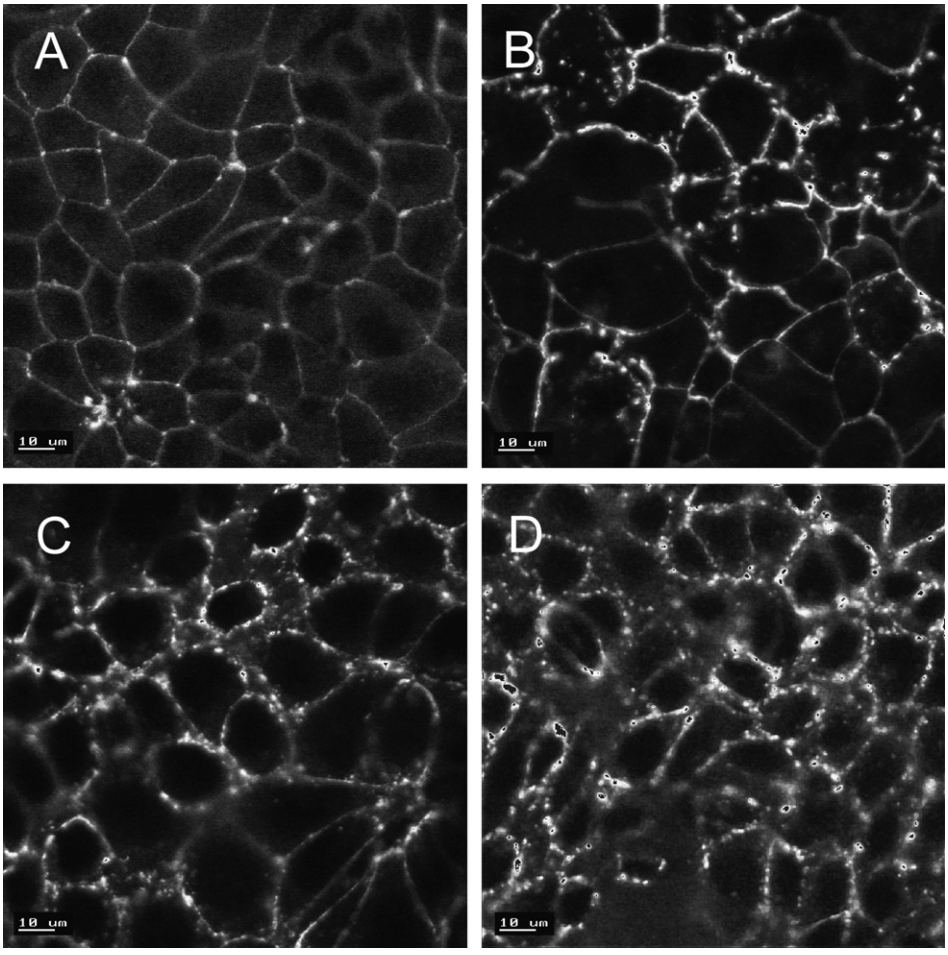

Fig. 6. CLSM images of Caco-2 cells labeled for occludin. (A) Maltose binding protein; (B) cytochalasin-D; (C) oxidised ZOT-CT; and (D) reduced ZOT-CT.

is stable at high pH, with a pI of 4.9, and ε for DTNB was 12400 M^{-1} cm^{-1}, close to the literature values [16]).

Confocal laser scanning microscopy (CLSM) investigation of the distribution of the tight junction (tj) transmembrane-associated protein occludin, the cytoplasmic tj associated protein ZO-1, and the perijunctional actin ring were made for polarized monolayers of Caco-2 cells. Polarized Caco-2 cells treated with MBP only (negative control) labelled for occludin, ZO-1 and F-actin showed a brightly stained continuous band circumventing each cell; i.e. the tj associated proteins were localized to the cell–cell boundaries, forming a typically sharp cobblestone-like organization (Figs. 6–8A) [17]. Following treatment with Cytochalasin D, an actin-disrupter, the distributions of occludin, ZO-1 and F-actin were largely modified: seen as fragmentation of the brightly stained cell boundaries, with areas of low and high intensity, indicating a loss and redistribution of the tj associated proteins (Figs. 6–8B). A similar reorganization of occludin and ZO-1 were observed as fragmentation of the brightly stained cell boundary following treatment with either oxidised or reduced ZOT-CT (Figs. 6C and D and 7C and D). However, cells stained for F-actin showed negligible change in the reorganization of the perijunctional actin ring upon incubation with reduced or oxidised ZOT-CT (Fig. 8C and D).

The transepithelial electrical resistance (TEER) is a commonly used variable to assess tj restricted paracellular permeability of polarized monolayers of Caco-2 cells. Following incubation with EDTA, the TEER decreased by 60% within 80 min (Fig. 9), demonstrating the loss of integrity in the tj protein complexes between the Caco-2 cells [18]. Incubation with MBP showed no change to the TEER over similar periods. The small, transient decreases in the TEER obtained for oxidised and reduced ZOT-CT were not statistically significant compared to the TEER data for MBP (Fig. 9). Following 1 h incubation of the cell monolayer with either EDTA or ZOT-CT, an equivalent increase in the apical to basolateral flux of dextran 4000 was observed (Fig. 10). After 2 h, an increase in flux was observed for EDTA but no further change was observed for ZOT-CT.

4. Discussion

ZOT has proven problematic to express and purify for structural characterisation [3], probably due to its predicted transmembrane domain (residues 215–239) [1]. Here, ZOT N- and C-terminal domains, avoiding residues 215–239, were expressed and purified to reasonable yield. The recombinant

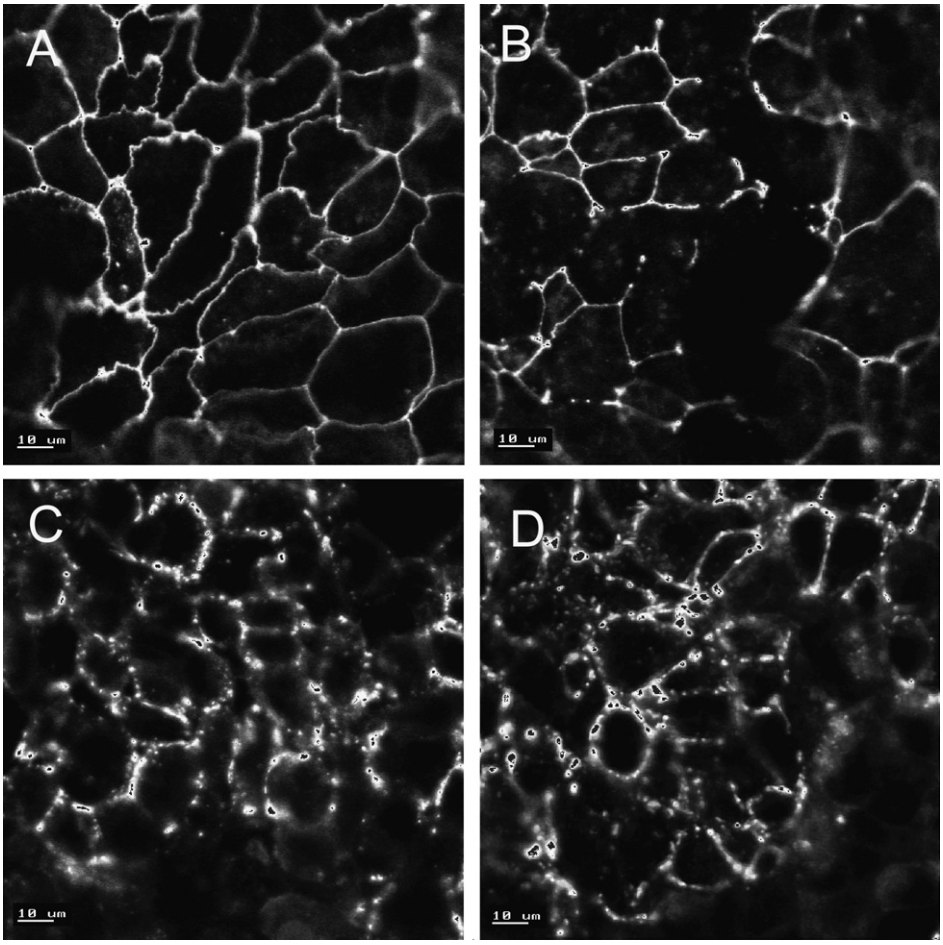

Fig. 7. CLSM images of Caco-2 cells labeled for ZO-1. (A) Maltose binding protein; (B) cytochalasin-D; (C) oxidised ZOT-CT; and (D) reduced ZOT-CT.

ZOT-NT is a highly basic protein (pI 9.9) with defined secondary structure, evinced by: (i) the presence of β-turn structure, implying a folded conformation rather than a disorganised polypeptide, (ii) a disulfide bond between Cys^{89} and Cys^{135} and (iii) the exposure to solvent of the Trp residues during equilibrium denaturation. The conformational stability of ZOT-NT is similar to other predominantly β-sheet/turn proteins domains, such as the 9th type III fibronectin domain ($\Delta G_{(H_2O)}$ 4.3 kcal/mol, $[GuHCl]_{\frac{1}{2}}$ 1.1 M) [19]. (No structural information is available for the pI family of proteins for further comparison.)

Although ZOT is distantly related to pI of filamentous bacteriophage f1, our investigations do not provide evidence that its modified A-motif functions as a Walker domain for the binding and hydrolysis of ATP [1]. Similarly, although pI is reduced by (host) thioredoxin for phage assembly [10], reduction of ZOT-NT had no effect on ATPase activity. Later studies on pI showed that its phage packing role also required a cytoplasmic amphipathic peptide leading into the membrane region (M^{241}KLTKIYLKKFSR) [9]. Since an analogous amphipathic sequence cannot be identified for the equivalent ZOT-NT residues (M^{202}YASTTTGKARDT), in retrospect, it may not be entirely surprising that neither is ATPase activity found. ZOT-NT may therefore simply orientate wild-type ZOT in the membrane such that ZOT-CT is cleaved within the periplasmic space for secretion into the intestinal milieu.

The evident reorganisation of the tj associated proteins occludin and ZO-1 following incubation of Caco-2 cell monolayers with ZOT-CT is consistent with previous analysis directed to the isolation of the putative binding domain (G^{290}RLCVQDG) [4]. Here we show that there is no requirement for a disulfide bridge between Cys^{288} and Cys^{293}, i.e. there is no stringent conformational requirement for recognition of ZOT-CT by its putative receptor. This may explain why small peptide mimics of the binding domain and partially folded ZOT maintain binding affinity for the ZOT receptor [3,4].

The absence of any significant fall in the TEER for the Caco-2 monolayer is supported by the observation that there was no reorganisation of the perijunctional actin ring for either oxidised or reduced ZOT-CT; for polarised epithelial cells it has been shown that the tj maintains its integrity for cells with organised perijunctional actin rings [20]. This is interesting because ZOT is known to increase the paracellular transport across Caco-2 monolayers of otherwise impermeable markers such as dextran [13]; the transient increase in the permeability of dextran across Caco-2 monolayers during incubation with ZOT-CT seen here (Fig. 10) is consistent with this previous

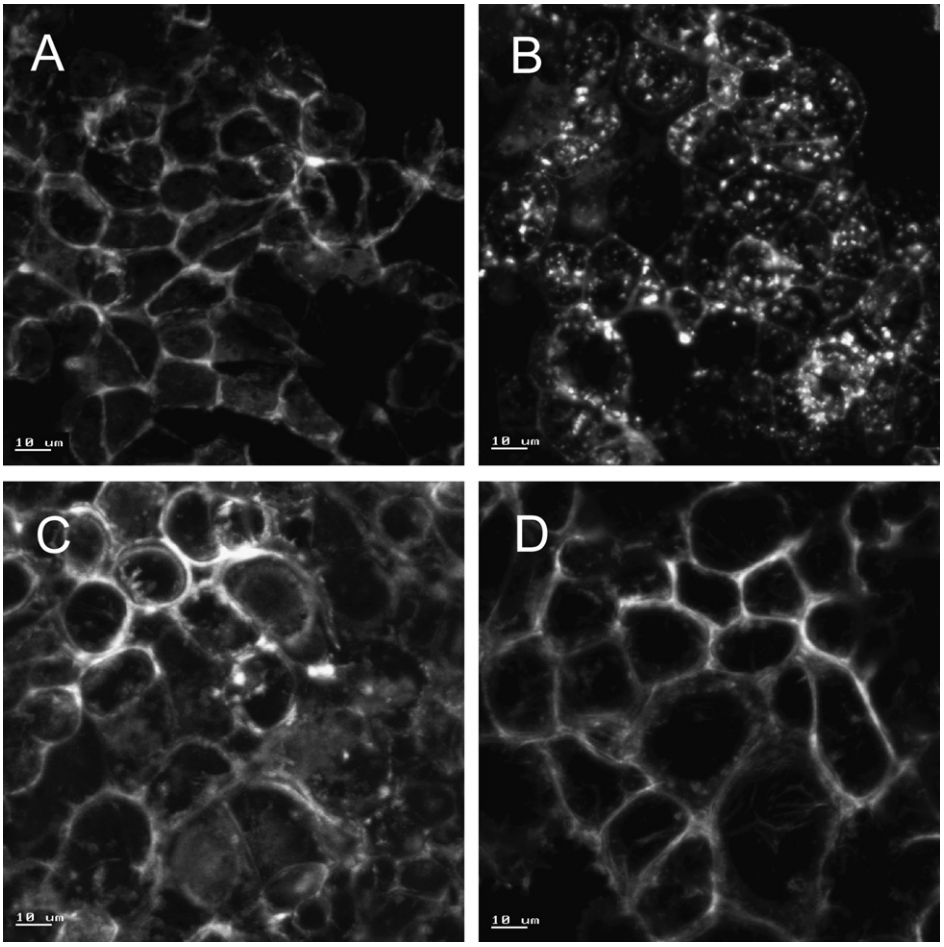

Fig. 8. CLSM images of Caco-2 cells labeled for F-actin. (A) Maltose binding protein; (B) cytochalasin-D; (C) oxidised ZOT-CT; and (D) reduced ZOT-CT.

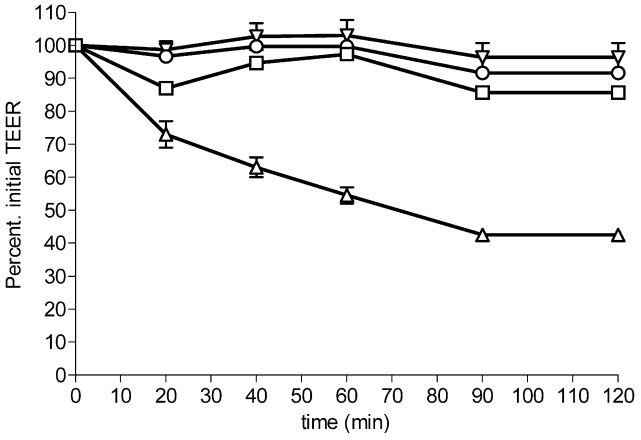

Fig. 9. TEER measured for Caco-2 cell monolayers grown in Transwell™ plates and treated with EDTA (△), MBP (▽), oxidised ZOT-CT (□) and reduced ZOT-CT (○).

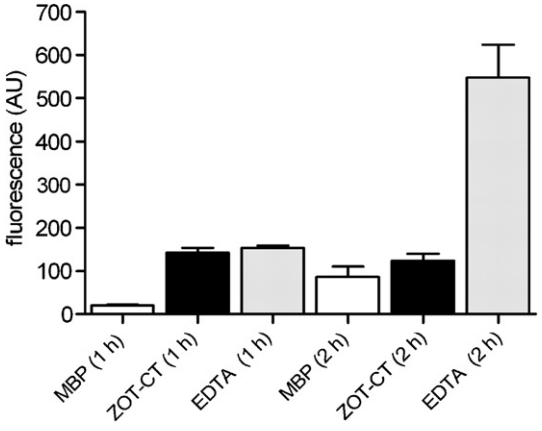

Fig. 10. Flux of FITC-dextran 4000 from apical to basolateral compartments across a confluent Caco-2 cell monolayer grown in Transwell™ plates, for co-incubation with MBP (clear bars), oxidised ZOT-CT (black bars) and EDTA (grey bars).

study. The ability of ZOT to increase paracellular transport of markers without altering the TEER is not actually unusual: the secreted autotransporter toxin, Sat, also increases paracellular flux across Caco-2 monolayers without a concomitant decrease in the TEER [21]. As here, Sat was observed to disrupt ZO-1 and (to a lesser extent) occludin but not F-actin. Whereas Sat is known to belong to the serine protease autotransporters, ZOT-CT does not align to any protein family. Futher

structure–function analysis of ZOT must therefore include isolation and cloning of the putative ZOT receptor.

Acknowledgements: We thank Elizabeth Goldie and Gail Connel for technical support with the CLSM. The Scottish Circular Dichroism Facility is funded by the BBSRC.

References

[1] Koonin, E.V. (1992) The second cholera toxin, Zot, and its plasmid-encoded and phage-encoded homologues constitute a group of putative ATPases with an altered purine NTP-binding motif. FEBS Lett. 312, 3–6.
[2] Fasano, A., Baudry, B., Pumplin, D.W., Wasserman, S.S., Tall, B.D., Ketley, J.M. and Kaper, J.B. (1991) Vibrio cholerae produces a second enterotoxin, which affects intestinal tight junctions. Proc. Natl. Acad. Sci. USA 88, 5242–5246.
[3] Lee, A., White, N. and van der Walle, C.F. (2003) The intestinal zonula occludens toxin (ZOT) receptor recognises non-native ZOT conformers and localises to the intercellular contacts. FEBS Lett. 555, 638–642.
[4] Di Pierro, M., Lu, R., Uzzau, S., Wang, W., Margaretten, K., Pazzani, C., Maimone, F. and Fasano, A. (2001) Zonula occludens toxin structure–function analysis. Identification of the fragment biologically active on tight junctions and of the zonulin receptor binding domain. J. Biol. Chem. 276, 19160–19165.
[5] Gorbalenya, A.E. and Koonin, E.V. (1989) Viral proteins containing the purine NTP-binding sequence pattern. Nucleic Acids Res. 17, 8413–8440.
[6] Baudry, B., Fasano, A., Ketley, J. and Kaper, J.B. (1992) Cloning of a gene (zot) encoding a new toxin produced by *Vibrio cholerae*. Infect. Immun. 60, 428–434.
[7] Guy-Caffey, J.K., Rapoza, M.P., Jolley, K.A. and Webster, R.E. (1992) Membrane localization and topology of a viral assembly protein. J. Bacteriol. 174, 2460–2465.
[8] Rapoza, M.P. and Webster, R.E. (1995) The products of gene I and the overlapping in-frame gene XI are required for filamentous phage assembly. J. Mol. Biol. 248, 627–638.
[9] Haigh, N.G. and Webster, R.E. (1999) The pI and pXI assembly proteins serve separate and essential roles in filamentous phage assembly. J. Mol. Biol. 293, 1017–1027.
[10] Russel, M. (1995) Moving through the membrane with filamentous phages. Trends Microbiol. 3, 223–228.
[11] Watson, N., Duncan, G., Annan, W.S. and van der Walle, C.F. (2006) A tetravalent RGD ligand for integrin-mediated cell adhesion. J. Pharm. Pharmacol. 58, 959–966.
[12] Greene Jr., R.F. and Pace, C.N. (1974) Urea and guanidine hydrochloride denaturation of ribonuclease, lysozyme, alpha-chymotrypsin, and beta-lactoglobulin. J. Biol. Chem. 249, 5388–5393.
[13] Cox, D.S., Raje, S., Gao, H., Salami, N.N. and Eddington, N.D. (2002) Enhanced permeability of molecular weight markers and poorly bioavailable compounds across Caco-2 cell monolayers using the absorption enhancer, zonula occludens toxin. Pharm. Res. 19, 1680–1688.
[14] Lobley, A., Whitmore, L. and Wallace, B.A. (2002) DICHROWEB: an interactive website for the analysis of protein secondary structure from circular dichroism spectra. Bioinformatics 18, 211–212.
[15] Sreerama, N. and Woody, R.W. (2000) Estimation of protein secondary structure from circular dichroism spectra: comparison of CONTIN, SELCON, and CDSSTR methods with an expanded reference set. Anal. Biochem. 287, 252–260.
[16] Riddles, P.W., Blakeley, R.L. and Zerner, B. (1983) Reassessment of Ellman reagent. Methods Enzymol. 91, 49–60.
[17] Menez, C., Buyse, M., Chacun, H., Farinotti, R. and Barratt, G. (2006) Modulation of intestinal barrier properties by miltefosine. Biochem. Pharmacol. 71, 486–496.
[18] Tomita, M., Hayashi, M. and Awazu, S. (1996) Absorption-enhancing mechanism of EDTA, caprate, and decanoylcarnitine in Caco-2 cells. J. Pharm. Sci. 85, 608–611.
[19] Annan, W.S., Fairhead, M., Pereira, P. and van der Walle, C.F. (2006) Emulsifying performance of modular β-sandwich proteins: the hydrophobic moment and conformational stability. Protein Eng. Des. Sel. 19, 537–545.
[20] Nusrat, A. et al. (1995) Rho protein regulates tight junctions and perijunctional actin organization in polarized epithelia. Proc. Natl. Acad. Sci. USA 92, 10629–10633.
[21] Guignot, J., Chaplais, C., Coconnier-Polter, M.H. and Servin, A.L. (2007) The secreted autotransporter toxin, Sat, functions as a virulence factor in Afa/Dr diffusely adhering *Escherichia coli* by promoting lesions in tight junction of polarized epithelial cells. Cell Microbiol. 9, 204–221.